

Electrochemistry in Nanostructured Inorganic Molecular Materials

Mary Elizabeth Williams and Joseph T. Hupp

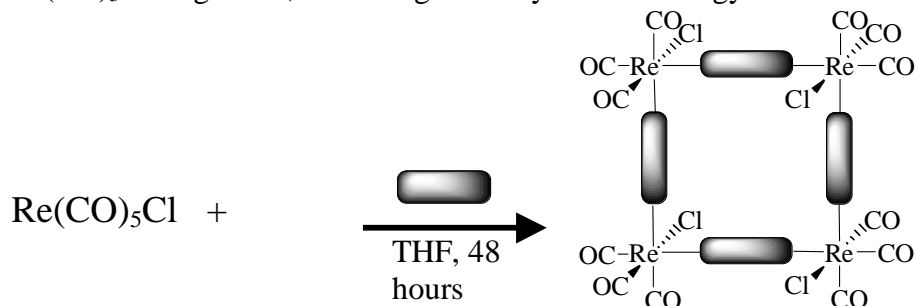
Department of Chemistry, Northwestern University, 2145 Sheridan Road, Evanston, IL 60208

Abstract

We have previously described the synthesis of a family of molecular ‘squares’ based on octahedral Re(I) coordination of difunctional bridging ligands. The size and chemical composition of the square cavity is highly tunable, and the inorganic cyclophanes are being actively studied in catalytic, separations, and sensing applications. Electrochemical techniques have been primary methods for characterization of the transport properties of thin films of the nanostructured materials. For example, cyclic voltammetry and rotating disk electrode voltammetry experiments have revealed size-selective permeation by redox probes, where the size cutoff is determined by the internal square dimensions. We have more recently begun to employ scanning electrochemical microscopy to spatially image micropatterned electrodes containing these thin film materials, simultaneously allowing us to obtain permeability data and topographical information. This paper describes data obtained by employing porphyrin-based molecular squares that feature chemically tailored cavities.

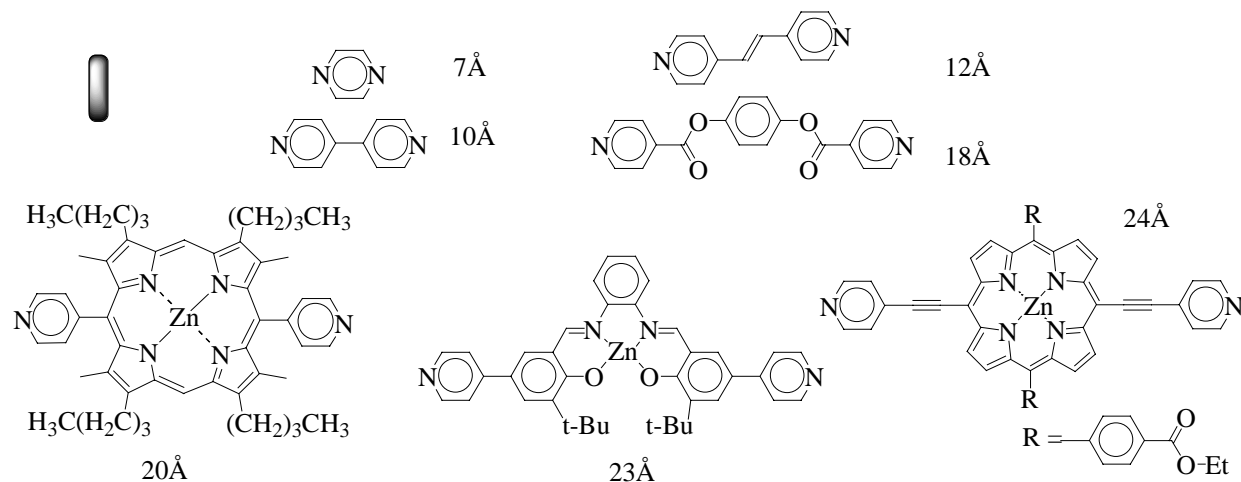
Introduction

We have actively been involved in the design and synthesis of molecular compounds capable of functioning in the solid state as microporous and mesoporous materials [1]. Among the applications, or potential applications, for such materials are membrane catalytic reactivity, environmental sensing of volatile hydrocarbons and heavy metals, and chemical separations [2]. To obtain the desired materials, we have prepared a family of inorganic complexes based on cis-coordination of $\text{Re}^{\text{I}}(\text{CO})_3\text{Cl}$ fragments, according to the synthetic strategy shown in Scheme 1.



Scheme 1. General synthetic scheme for the rhenium-based molecular squares. Although only one isomer, with respect to carbonyl and chloro ligand positions, is shown, it is believed that all four of the possible isomers are obtained.

Using a series of difunctional pyridine-based bridging ligands, some of which are shown in Scheme 2, we have demonstrated that the size of the molecular square (the spacing between Re corners) may be varied from 7 to 24 Å [1]. All of the molecular squares possess $\text{Re}(\text{CO})_3\text{Cl}$



Scheme 2. Structures of the pyridine-based ligands: (A) pyrazine; (B) 4,4'-bipyridine; (C) 4,4'-bis(pyridyl) ethylene; (D) dipyrindyl ; (E) 2,8,12,18-tetrabutyl-3,7,13,17- tetramethyl-5,15-bis(4-pyridyl) Zn^{II} porphyrin; (F) bis(3-*tert*-butyl-5-(4-pyridyl) salicylidene)-1,2-phenylenediaminozinc(II); (G) 10,20-bis(4-ethoxy phenyl)-5,15-bis(ethynyl-4-pyridyl) Zn^{II} porphyrin.

corners and thus are neutral in charge, making them soluble and processible in common organic solvents yet completely insoluble in aqueous environments.

An early structural observation/confirmation [1c], derived from single-crystal x-ray diffraction measurements, was that bridging ligands serve to define molecular cavities. Examples of space-filled diagrams based on x-ray crystallographic data are shown in Figure 1. The molecular squares pack in such a way that substantive interstitial cavities do not exist. In

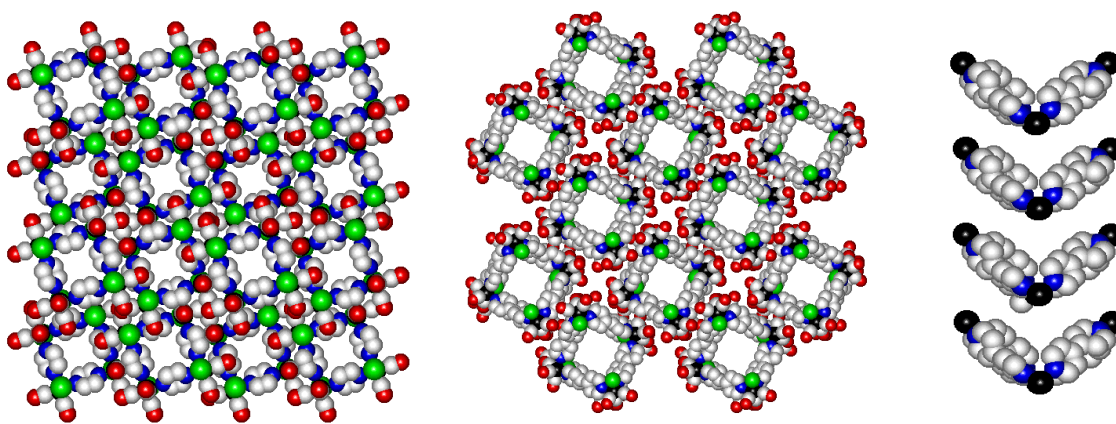


Figure 1. Space-filled diagrams based on the x-ray crystal structures of the (A) pyrazine molecular square and (B) 4,4'-bipyridine molecular square. (C) Side view of the 4,4'-bipyridine molecular square; the carbonyl ligands and the hydrogen and chlorine atoms have been omitted for clarity.

addition, the vertical stacking of the molecules results in semi-infinite, nanoscale channels that extend through the crystal. The importance of the lack of charge-compensating counterions is

again highlighted, since their presence could potentially fill the molecular cavities and block transport of other species.

This report presents experimental results based on electrochemical techniques, including cyclic voltammetry and scanning electrochemical microscopy, examining the molecular sieving properties of microporous thin films composed of porphyrinic squares. By quantitatively assessing permeabilities within the thin films, we are able to evaluate the extent to which chemical control of molecular sieving properties can be achieved while retaining high molecular fluxes.

Experimental.

The synthesis of the porphyrinic ligands and the molecular squares has been described previously [1]. Ultrapure (18M Ω) water (Millipore) was employed for all aqueous solutions. All other chemicals were commercially available and used as received.

Electrochemical experiments were performed with a CH Instruments Model 900 scanning electrochemical microscope and potentiostat. The scanning electrochemical microscope (SECM) microelectrode tips consisted of 8 μm diameter carbon fibers, insulated as described previously [3]. Indium tin oxide coated glass slides (Delta Technologies) were photolithographically patterned as before [3].

Results and Discussion.

When cast on electrode surfaces, thin films of the molecular squares have been shown to exhibit size-selective permeability toward redox-active molecular probes [1]. Figure 2 depicts schematically molecular sieving by a thin film of porphyrinic molecular square, where only molecular probes with dimensions smaller than the materials' channel dimensions are able to permeate the film.

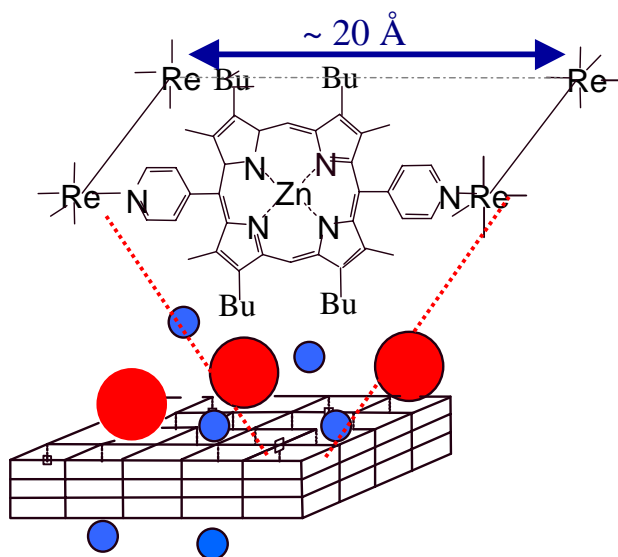


Figure 2. Cartoon depiction of molecular sieving by a thin film of the porphyrinic molecular square.

the mesoporous material, using cyclic voltammetry (CV) in a solution containing two redox redox probes of varying sizes. A CV response obtained using an ITO electrode containing a 100

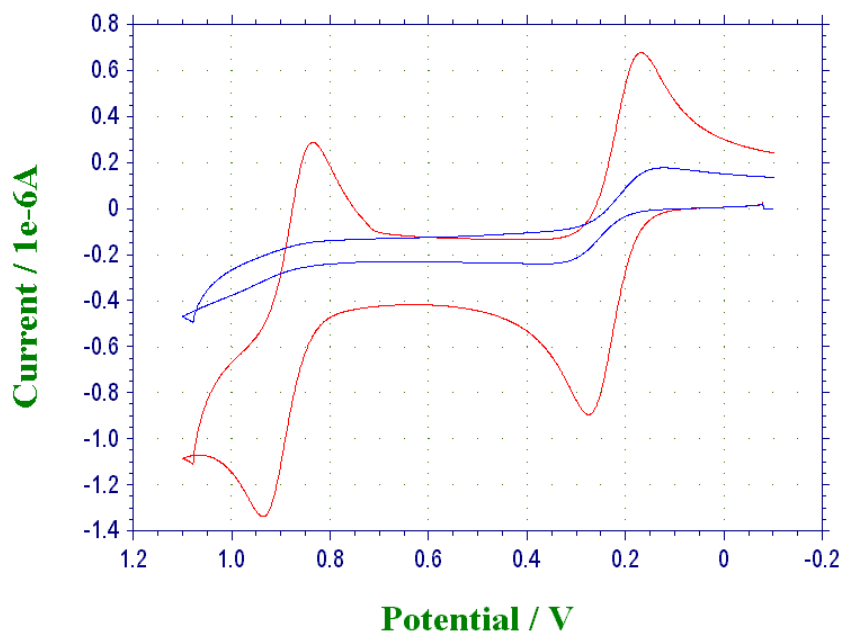


Figure 3. Cyclic voltammetry of a bare electrode (—) versus a film-covered (190 nm thick of **A**) electrode (—), in an aqueous solution containing 1.0 mM $\text{Fe}(\text{bathophenanthroline}(\text{SO}_3)_2)_3^{4+}$ and 1.1 mM FcMeOH .

nm thick film of the porphyrin square, compared to the bare electrode response in the same solution, is shown in Figure 3. The lack of voltammetric response for the larger of the two redox species ($[\text{Fe}(\text{bphen}(\text{SO}_3)_2)_3]^{4+}$) is attributed to its complete exclusion from the porphyrinic film. We consistently observe that the size cutoff for permeation of the films corresponds with the known dimensions of the molecular-square cavities [1].

The most versatile molecular squares are the Zn^{II} macrocycle-based compounds, since the

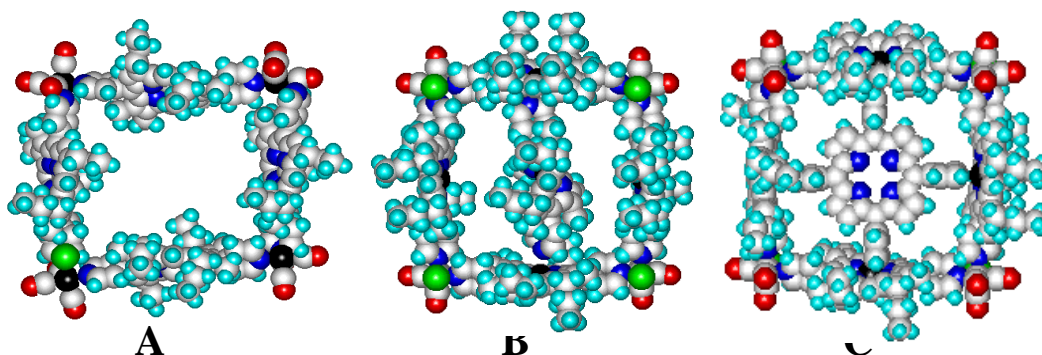


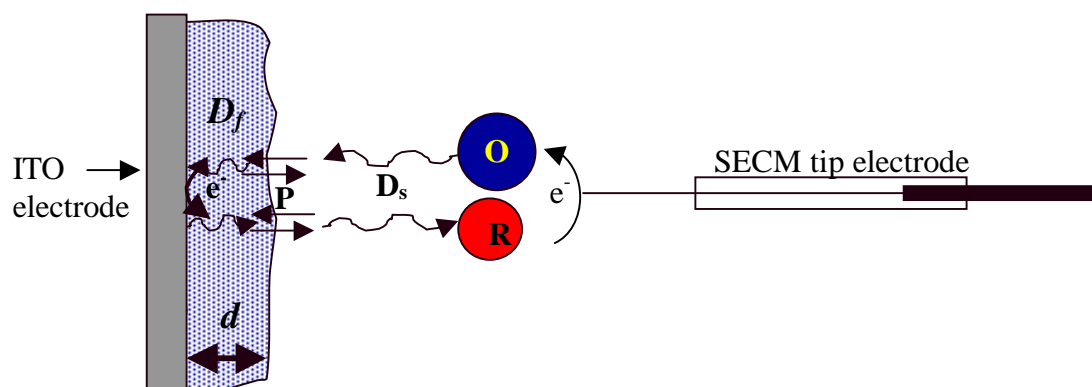
Figure 4. Drawings of the porphyrinic molecular squares: (A) underivatized square; (B) porphyrin square with a bound dipyriddy porphyrin; (C) porphyrin square with a bound tetrapyriddy porphyrin.

metal center may axially coordinate an additional ligand. We have utilized this strategy to change the size, chemical nature, and catalytic behavior of the cavities [4]. Shown in Figure 4 are space-filled diagrams (models, not x-ray structures) of a porphyrin molecular square which has been modified by coordination to dipyrindyl or tetrapyrindyl porphyrins. The binding constants of these ligands within the square cavity are ca. 10^6 and 10^7 M^{-1} , respectively, in solution environments (CH_2Cl_2) and likely greater in thin film (aqueous) environments [1]. By binding a fifth porphyrin, the intramolecular cavities are divided into two ca. 8×18 Å channels and four ca. 5×5 Å openings, in assemblies **B** and **C**, respectively.

Although cyclic voltammetric responses (such as in Figure 3) imply a high degree of control over molecular sieving, we find that quantitative transport rate measurements are most reliably obtained via Scanning Electrochemical Microscopy (SECM) measurements. SECM is capable of simultaneously providing microscopic topographical images and film-based molecular flux measurements for redox-active probe molecules [5]. Scheme 3 depicts the flux of a redox-active molecular species during SECM in feedback mode [6]: to yield an SECM current, the redox probe must first diffuse through solution, partition across the film/solution interface, and diffuse through the film to the underlying electrode surface. After electron transfer at the electrode interface, the oxidized (or reduced) redox probe diffuses back out of the film and into solution to the SECM tip. The coupling of diffusion and partitioning in the overall mass transport of the redox probe is well understood. For the current obtained by the SECM tip microelectrode in feedback, we are able to write a simplified expression [3]

$$\left(\frac{i_{tip}}{i_{film}} \right)^{-1} = 1 + \frac{4\pi r P D_f C}{D_s d} \quad (1)$$

where the tip current obtained over the film-covered substrate (i_{film}) is normalized to that obtained at identical height over a bare ITO surface (i_{tip}) and r is the microelectrode tip radius (see Scheme 3 caption for other constants). (Note that current, in this experiment, is simply an electrochemical measurement of probe-molecule flux.) For thicker films, which require the



Scheme 3. Coupling of solution-phase and film-based diffusive transport of redox probes during the SECM experiment. D_s and D_f are the solution and film diffusion coefficients of the redox species, respectively; d is the film thickness; P is the redox-probe partition coefficient.

redox probe to diffuse through greater distances, less current is observed. An inverse-linear relationship between the normalized current and film thickness is predicted based on the permeation/diffusion model, under conditions where diffusion, rather than phase partitioning, is rate-determining.

Figure 5 shows an example of an SECM image of a photolithographically patterned ITO electrode using the redox mediator $\text{Ru}(\text{NH}_3)_6^{3+}$. The image shows a regular array of $50\ \mu\text{m} \times 50\ \mu\text{m}$ bright regions that are separated by $50\ \mu\text{m}$. In this experiment, the ITO electrode was held at

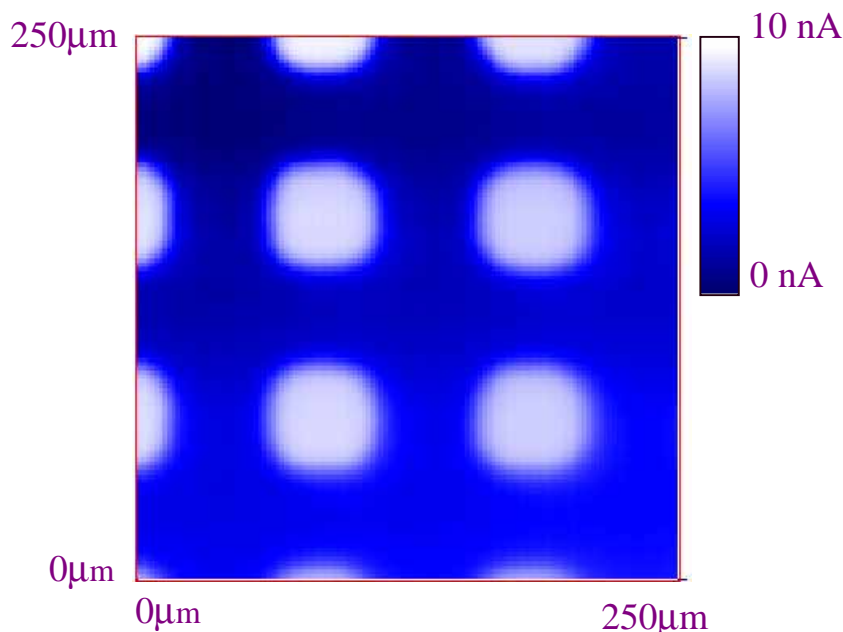


Figure 5. Scanning Electrochemical Microscopy image of a photolithographically patterned ITO electrode, obtained using a $8\ \mu\text{m}$ diameter carbon fiber electrode in a $3\ \text{mM}$ aqueous solution of $\text{Ru}(\text{NH}_3)_6^{3+}$. SECM tip potential is $0\ \text{V}$ and the ITO electrode potential is $-0.35\ \text{V}$ vs. SCE.

$-350\ \text{mV}$ and thereby used to reduce the $\text{Ru}(\text{NH}_3)_6^{3+}$; the SECM tip was held at $0\ \text{V}$ vs. SCE; the $\text{Ru}(\text{NH}_3)_6^{3+/2+}$ formal potential is $-0.25\ \text{V}$ vs. SCE. The bright areas in the image are thus due to the re-oxidation of $\text{Ru}(\text{NH}_3)_6^{2+}$ and correspond to the conductive areas on the patterned ITO surface. We utilize these micropatterned arrays to rapidly assess and maximize the experimental parameters, to collect a large amount of data on separate micron-sized areas of thin films, and to provide a reference registry for separate, external measurements such as atomic force microscopy.

While in typical experiments thin films are prepared by spin coating the molecular material to produce films of uniform thickness, one of the goals of the SECM experiment was to demonstrate the ability to assess multiple types of materials on the same micropatterned array. In the SECM images in Figure 6, thin films of the three porphyrinic squares (Figure 4) were cast onto the same ITO micropatterned electrode. Images were obtained of these films using a series

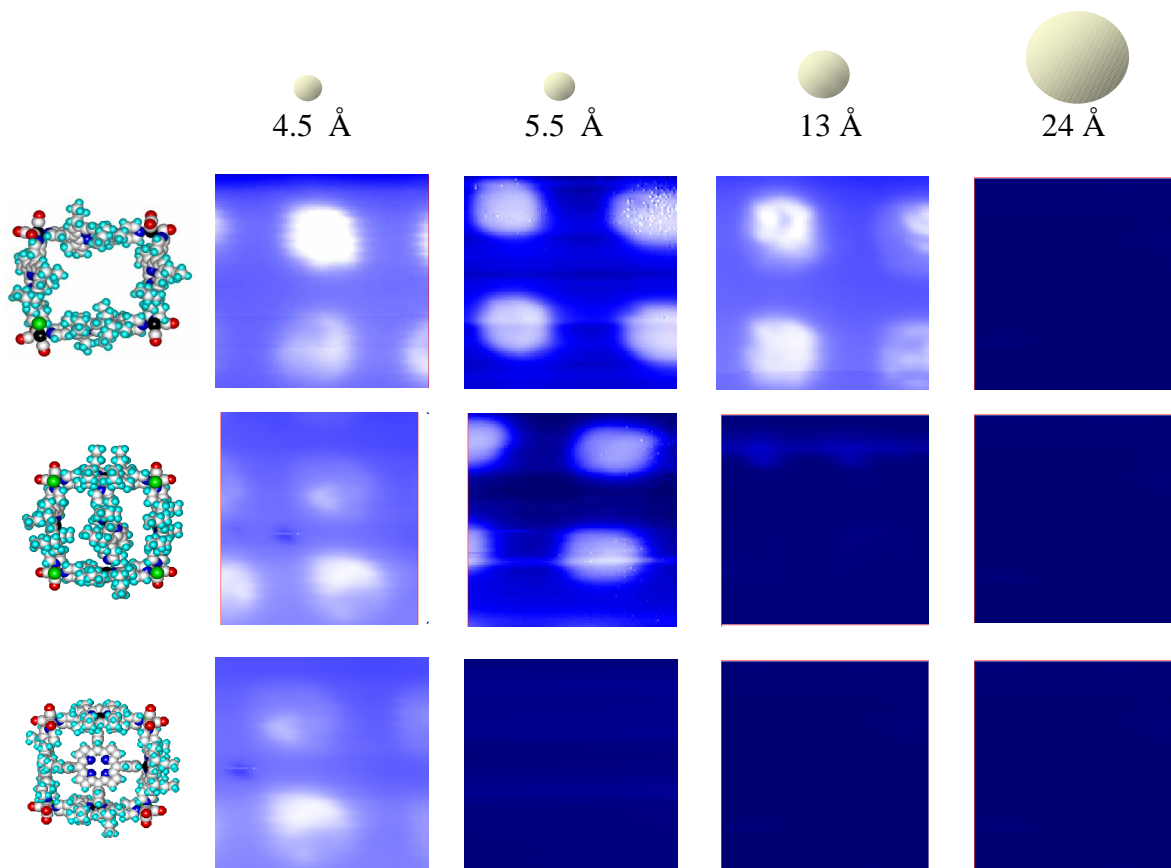


Figure 6. Series of SECM images obtained on a single ITO patterned substrate, containing films of the three indicated porphyrinic squares. The redox probes used to obtain the images are FcMeOH (4.5 Å), $\text{Ru}(\text{NH}_3)_6^{3+}$ (5.5 Å), $\text{Fe}(\text{phen})_3^{2+}$ (13 Å) and $\text{Fe}(\text{bphen}(\text{SO}_3)_2)_3^{4+}$ (24 Å).

of redox-active molecular probes (see Figure 6 caption) to assess experimentally the extent to which control over size cutoffs for molecular transport could be exercised via coordination of a fifth porphyrin ligand [7]. It is immediately apparent from the images that SECM tip currents are obtained only for redox-active probe molecules whose dimensions are smaller than the molecular square cavity, modified cavity, or port dimensions. The lack of images for the larger redox probes is attributed to their exclusion from the films, and is consistent with the chemically-defined microporosity of these materials. It is important to note that because the films are small in area ($2.5 \times 10^{-5} \text{cm}^2$, versus 0.1cm^2 in the cyclic voltammetry experiment in Fig. 3), it is much more straightforward to obtain pinhole-free domains, so that the measured fluxes may be attributed to film permeation rather than pinhole diffusion. The remarkable size-selectivity of these materials is highlighted by the film of porphyrin assembly C, for which images were obtained for the 4.5 Å diameter FcMeOH but not for the 5.5 Å diameter $\text{Ru}(\text{NH}_3)_6^{3+}$.

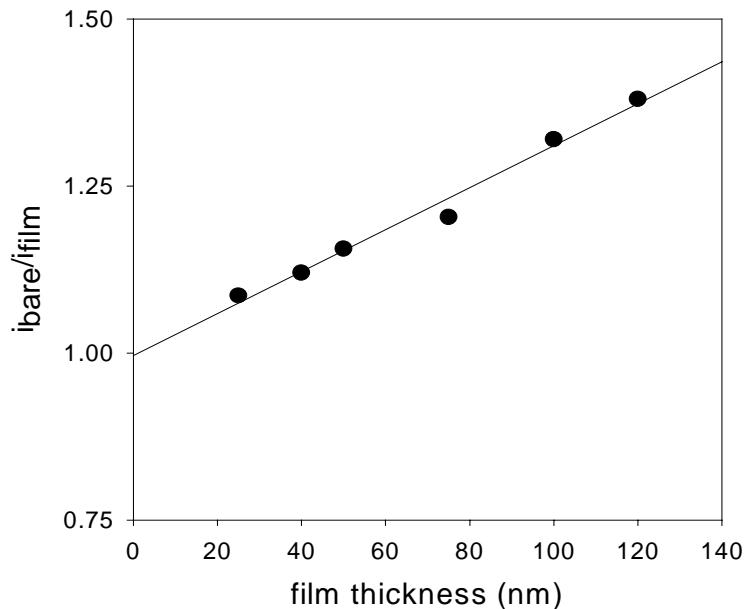
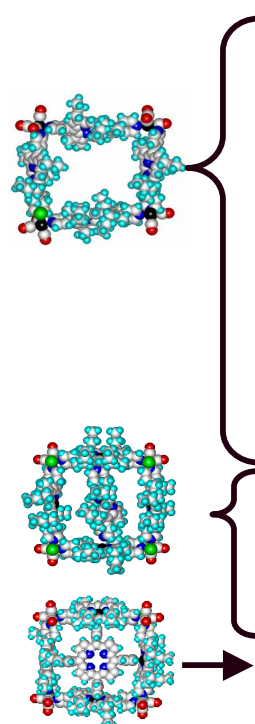


Figure 7. Plot of the normalized SECM tip response for a series of porphyrin square thin films using the indicated redox probes.

When a meso- or microporous thin film is spin-coated onto the micropatterned array, the current response at the SECM tip is attenuated according to Eq 1. To determine accurately the molecular probe permeability, PD_f , a plot such as shown in Figure 7 is constructed using the current response for several films of varying thickness. One of the benefits of utilizing the micropatterned array platforms is that large amounts of data are obtained for a particular film. Thus, each data point in Figure 7 represents the average of 140 or more separate measurements. Using the slopes of the plots shown in Figure 7 and the known solution diffusion coefficient and concentration of the redox probes, one can determine with remarkable precision PD_f value for the probe molecule in the microporous porphyrinic material. Table 1 summarizes data for a broader study, detailed elsewhere [8], involving a family of materials and range of probes of varying size.

Table 1. Redox Probe Permeabilities in Porphyrinic Molecular Squares



Redox Mediator	Diameter (Å)	PD _f (cm ² /s) x 10 ⁹
FcMeOH	4.5	14.5 + 0.1
Ru(NH ₃) ₆ ³⁺	5.6	25.0 + 0.1
Fe(CN) ₆ ⁴⁻	6	11.1 + 0.04
Co(bpy) ₃ ²⁺	12	3.64 ± 0.02
Fe(phen) ₃ ²⁺	13	1.89 ± 0.03
Fe(bphen(SO ₃) ₂) ₃ ⁴⁻	24	0
FcMeOH		9.9 ± 0.5
Ru(NH ₃) ₆ ³⁺		18 ± 1
Fe(CN) ₆ ⁴⁻		7.2 ± 0.7
FcMeOH		6.5 ± 0.9

Acknowledgments. We gratefully acknowledge the contributions of graduate students Katy Splan, Melinda Keefe, Melissa Merlau, and Aaron Massari. We thank the National Science Foundation for current support and the Office of Naval Research for earlier support of our research.

References.

- [1] (a) Slone, R. V.; Hupp, J. T. *Inorg. Chem.* 36, 5422 (1997). (b) Belangér, S.; Hupp, J. T. *Angew. Chem. Intl. Ed.* 38, 2222 (1999). (c) Belangér, S.; Hupp, J. T.; Stern, C. L.; Slone, R. V.; Watson, D. F.; Carrell, T. G. *J. Am. Chem. Soc.* 121, 557 (1999). (d) Belangér, S.; Anderson, B. C.; Hupp, J. T. *Proc. - Electrochem. Soc.* 98-26, 208 (1999). (e) Slone, R. V.; Benkstein, K. D.; Belangér, S.; Hupp, J. T.; Guzei, I. A.; Rheingold, A. L. *Coord. Chem. Rev.* 171, 221(1998). (f) Keefe, M. H.; Morris, G. A.; Hupp, J. T. Nguyen, S. T., unpublished studies.

-
- [2] (a) Keefe, M. H.; Slone, R. V.; Hupp, J. T.; Czaplewski, K. F.; Snurr, R. Q.; Stern, C. L. *Langmuir* 16, 3964 (2000). (b) Keefe, M. H.; Benkstein, K. D.; Hupp, J. T. *Coord. Chem. Rev.* 205, 201 (2000). (c) Merlau, M. L.; Grande, W. J.; Nguyen, S. T.; Hupp, J. T. *J. Mol. Cat. A* 156, 79 (2000).
- [3] Williams, M. E.; Stevenson, K. J.; Massari, A.; Hupp, J. T. *Anal. Chem.* 72, 3122 (2000).
- [4] Belangér, S.; Keefe, M. H.; Welch, J. L.; Hupp, J. T. *Coord. Chem. Rev.* 190-192, 29 (1999).
- [5] (a) Bard, A. J.; Denault, G.; Lee, C.; Mandler, D.; Wipf, D. O. *Acc. Chem. Res.* 23, 357 (1990). (b) Bard, A. J.; Fan, R. -R. F.; Mirkin, M. V. In *Electroanalytical Chemistry*, Bard, A. J., Ed.; Marcel Dekker: New York, 1994, Vol. 18, pp. 243.
- [6] Feedback refers to the flux of the redox mediator, where electrode currents observed at the SECM tip electrode are enhanced by the proximity of the tip to the conductive sample surface.
- [7] To prepare a sample with three materials on the same micropatterned platform, solutions of the porphyrinic squares were drop-cast onto separate areas. This method does not produce films of uniform thickness, which is apparent in the images by the variations in current for individual 50 micron areas.
- [8] Williams, M. E.; Hupp, J. T. submitted to *J. Phys. Chem. B* (2001).